SCIENCE CHINA
Technological Sciences

•Review•

November 2021 Vol.64 No.11: 2347–2359
https://doi.org/10.1007/s11431-020-1833-4

Ultrathin molybdenum disulfide (MoS_2) film obtained in atomic layer deposition: A mini-review

YANG JunJie, XING YouQiang, WU Ze, HUANG Peng & LIU Lei*

School of Mechanical Engineering, Southeast University, Nanjing 211189, China

Received November 16, 2020; accepted April 12, 2021; published online July 21, 2021

Atomic layer deposition (ALD) as a flexible surface-controlled fabrication technique has attracted widespread interest in numerous nanotechnology applications, which can obtain ultrathin or two-dimensional molybdenum disulfide (2D MoS_2) films. The ALD technique possesses the characteristics of precise thickness control, excellent uniformity, and conformality, relying on the self-limiting surface reaction. In this mini-review, the knowledge about the fabrication mechanisms and applications of ALD prepared MoS_2 films is reviewed. The surface reaction pathway about ALD synthesis MoS_2 is elaborated, and the corresponding factors causing saturation adsorption are discussed. Two possible growth mechanisms of ALD-MoS_2 film based on the building blocks and MoS_2 islands are compared. For both, the deposition process of MoS_2 can be divided into two stages, heterogeneous deposition stage and homogeneous deposition stage. The mismatch between the as-deposited MoS_2 in the heterodeposition and the lattice structure of the substrate surface is a key factor leading to the poor crystallinity of as-deposited MoS_2. In addition, the extensions of ALD MoS_2 technique to improve the as-deposited film quality are discussed. Finally, the applications of ALD deposited MoS_2 film are summarized, and future perspectives are outlined.

atomic layer deposition, MoS_2 film, self-limiting surface reaction, growth mechanism

Citation: Yang J J, Xing Y Q, Wu Z, et al. Ultrathin molybdenum disulfide (MoS_2) film obtained in atomic layer deposition: A mini-review. Sci China Tech Sci, 2021, 64: 2347–2359, https://doi.org/10.1007/s11431-020-1833-4

1 Introduction

Transition metal dichalcogenides (TMDs), mainly represented by molybdenum disulfide (MoS_2), have attracted worldwide attention for the last few years [1]. 2D MoS_2 consists of a sandwich structure in which a layer of Mo atoms is hexagonally packed in the middle, and the top and bottom are a layer of S atoms, respectively [2]. In a MoS_2 layer, one Mo atom is connected with six S atoms by covalent bonds, while MoS_2 layers can be stacked into a layered crystalline structure by van der Waals force [3]. When the bulk of MoS_2 is reduced to a single layer, an indirect bandgap (1.3 eV) will be transformed to a direct bandgap (1.8 eV) [2]. Depending on its unique and tunable electronic properties, 2D MoS_2 has been employed in many applications such as transistors [4–6], spintronics [7], photovoltaics [8], sensors [9], biomedical sciences [10], and nanotribology [11]. The fabrication of 2D MoS_2 films with precise thickness control, excellent uniformity, and conformality is still challenging.

The preparation of 2D MoS_2 can usually be summarized as a top-down method and a bottom-up method [12]. Mechanical exfoliation as a top-down approach has first been developed to prepare ultrathin MoS_2, mainly being used for research purposes instead of large-scale productions [13]. Comparatively speaking, bottom-up approaches such as various chemical vapor deposition methods [14–16] show strong competitiveness and good application prospects in the future large-scale production of ultrathin films. The methods of chemical vapor deposition (CVD) [14] and metal-organic chemical vapor deposition (MOCVD) [15] usually involve a

*Corresponding author (email: liulei@seu.edu.cn)

direct gas phase reaction between precursors. Therefore, these methods have a higher deposition temperature or a strong dependence on the type of substrate. However, the method of atomic layer deposition (ALD) [16] replaces the direct chemical reaction with two half-reactions [17], which seems the most suitable for the controllable fabricating 2D MoS_2 [12,18,19]. In this way, the synthesized MoS_2 films can exhibit precise layer controllability, wafer-scale uniformity and homogeneity, and excellent conformality.

Since 2D MoS_2 films were firstly prepared by Tan et al. [16] through the ALD method with $MoCl_5$ and H_2S as precursors, the exploration of ALD technology has been developed in many ways, such as the discovery of novel Mo or S precursors. Immediately afterward, Jin et al. [25] used $Mo(CO)_6$ and $CH_3S_2CH_3$ precursors to decrease the deposition temperature of ALD preparation of MoS_2 effectively. Later, the literature has reported other innovative precursors, such as Mo precursors of $Mo(NMe_2)_4$ [26] and S precursors of H_2S plasma [27]. In addition, some advanced techniques to enhance the quality of ALD synthesis MoS_2 films have also been developed, such as post-deposition annealing [22], substrate surface pretreatment [28], plasma-enhanced atomic layer deposition (PEALD) [29,30], and the method combined the features of CVD and ALD [24,31] (Figure 1). Especially for the last, MoS_2 can be prepared via CVD sulfurizing MoO_3 film deposited by ALD. Thus the crystallinity of MoS_2 deposited by combining the advantages of both methods is further improved.

Although numerous successful applications of ALD deposited MoS_2 film have been practiced, the most essential physical or chemical processes that control the process of ALD deposited MoS_2 are not thoroughly understood yet. To achieve a greater degree of awareness about the fabrication of MoS_2 film using ALD, an overview about the fabrication mechanisms of MoS_2 film deposited by ALD technique, especially for its surface chemistry and the detailed process, is so desperately needed. However, there have been numerous reviews on the ALD technique or 2D MoS_2 [12,18,19,32–37]. Therefore, this mini-review focuses on the fabrication mechanisms of ALD preparation of MoS_2, such as the self-limiting surface reaction and growth mechanisms.

2 Fabrication mechanisms

2.1 ALD cycle and precursors

Generally, one complete ALD cycle of MoS_2 on the substrate surface consists of four steps [16,20] (Figure 1): (1) Mo precursors are injected into the vacuum chamber and adsorbed by the hydroxyl groups terminated on the surface of the substrate; (2) the remaining Mo precursors in the reaction chamber are purged by nitrogen flows; (3) S precursors are injected into the vacuum chamber and react with the Mo precursors adsorbed on the surface of the substrate; (4) the vacuum chamber is purged by nitrogen flows again. Steps 1–4 constitute one complete ALD MoS_2 cycle, which consists of two half-reactions (steps 1 and 3) and two evacuations (steps 2 and 4). These steps are repeated with each cycle to produce a definite thickness of MoS_2.

The Mo and S precursors, which are never present at the

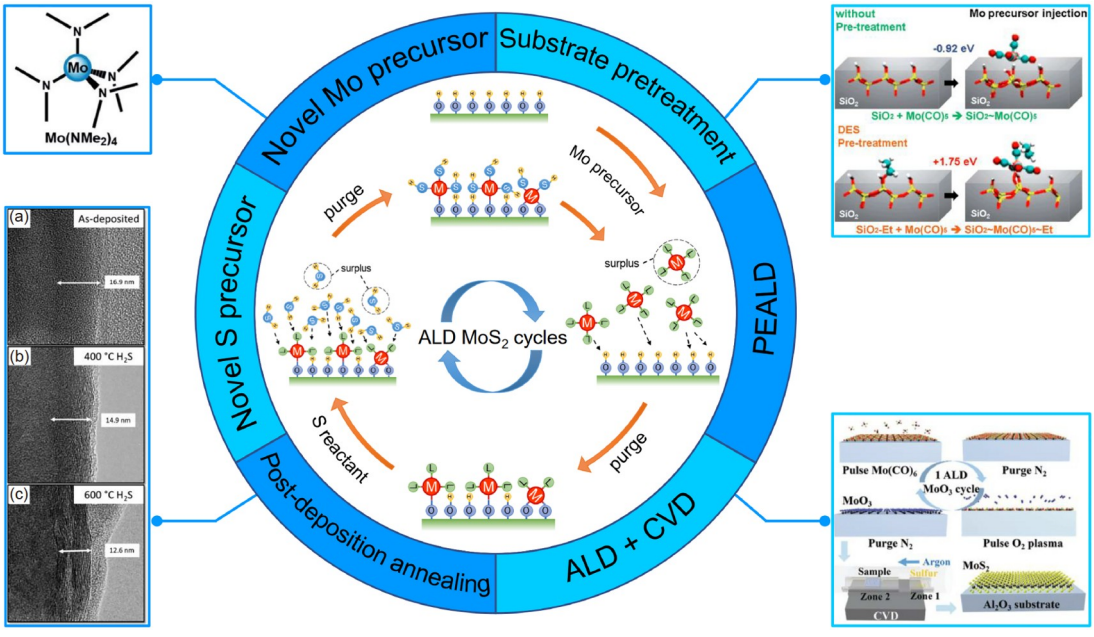

Figure 1 (Color online) Schematic representation of the process of ALD and the techniques to improve the quality of ALD synthesis MoS_2 film. Reprinted with permission from ref. [20], Copyright 2015, John Wiley and Sons. Ref. [21], Copyright 2017, John Wiley and Sons. Ref. [22], Copyright 2018, American Chemical Society. Ref. [23], Copyright 2017, John Wiley and Sons. Ref. [24], Copyright 2017, John Wiley and Sons.

same time, cannot directly react in the reaction chamber due to the separation of the purge steps. The precursors react only with the active site on the substrate surface in a self-limiting surface reaction process. The two half-reaction sequences could avoid uncontrolled straightforward gas phase reactions, which is essentially different from other vapor deposition methods (such as CVD) based on the direct gas-phase chemical reaction between two precursors [38]. ALD reaction sequences are independent of transport due to the self-limiting surface reaction, which can concisely distinguish ALD from other chemical vapor deposition techniques which depend on the type and rate of vapor precursor transport [39].

Although most of the MoS_2 films deposited by ALD have a similar binary process, the difference of precursor makes each one ALD MoS_2 process has its own hallmarks. Generally, the precursor should be thermally stable and volatile at the reaction temperature so that the precursor is highly reactive toward the active site on the surface of the substrate [40], especially the surface of semimetal or metal [41]. Some examples reported in the literature are summarized in Table 1.

The precursors can be divided into homoleptic precursors (all ligands identical) and heteroleptic precursors (not all ligands identical). At present, the research content about the precursors of ALD MoS_2 can be summed up in two aspects of attempts. One effort is to find active precursors with high thermal stability. The synthesis of heteroleptic precursors is an availability strategy to tailor the properties of precursors. For instance, $(N^tBu)_2(NMe_2)_2Mo$ as a heteroleptic precursor is used to promote the quality of the film in the ALD synthesis MoS_2, in which Mo precursor can exhibit better thermal stability at high deposition temperatures when its oxidation state is lower than 4 [40]. Another effort is to decrease the deposition temperature by using a new Mo precursor or S precursor. For example, the deposition temperature of $MoCl_5$ processes is usually more than 300°C, but the deposition temperature of $Mo(NMe_2)_4/HS(CH_2)_2SH$

Table 1 Summary about the Mo and S precursors for ALD-made MoS_2 film processes

Mo precursor	S precursor	Growth temperature (°C)	Grain	Grain after annealing	Ref.
$MoCl_5$	H_2S	300	Amorphous	~2 μm	[16]
		420–480	~20–100 nm	–	[42]
		300	Crystalline	–	[43]
		200–420	10–25 nm	–	[5]
	HMDST[a)]	375	–	Crystalline	[44]
		300–350	Amorphous	Crystalline	[45]
		350	Amorphous	Crystalline	[6]
$Mo(CO)_6$	H_2S	120–200	Amorphous	–	[46]
		120–200	Amorphous	Crystalline	[47]
	H_2S plasma	175–225	~20 nm	–	[48]
		200	~100 nm	–	[49]
		200	~6–10 nm	~14 nm	[27]
	$CH_3S_2CH_3$	60–140	Amorphous	Crystalline	[25]
		100	Amorphous	–	[50]
		100	Amorphous and nanocrystalline	–	[51]
	HMDST[a)]	150	Amorphous	Crystalline	[52]
$Mo(NMe_2)_4$	H_2S	60	Amorphous	Crystalline	[21]
	$HS(CH_2)_2SH$	50	Amorphous	~20 nm	[26]
$Mo(thd)_3$	H_2S	300	~10–30 nm	–	[53]
MoF_6	H_2S	200	Amorphous	4–10 nm	[22]
		200	Amorphous	50–100 nm	[54]
		700	Crystalline	–	[55]
$(N^tBu)_2(NMe_2)_2Mo$[b)]	H_2S	275	0.106 nm	–	[56]
		100–300	Amorphous	Crystalline	[57]
	$(CH_3)(CH_2)_2SH$	350	Amorphous	Crystalline	[58]
	H_2S-Ar plasma	250	~5–7 nm	–	[29]
	H_2+H_2S+Ar plasma	200–450	Amorphous to polycrystalline	–	[30]

a) HMDST is hexamethyldisilathiane; b) $(N^tBu)_2(NMe_2)_2Mo$ is bis(t-butylimino)bis(dimethylamino)molybdenum.

process is only 50°C [26]. This means MoS_2 can be deposited on the polymeric substrates and photoresists. According to the data in Table 1, $Mo(CO)_6$ and H_2S are obviously the most used precursors of MoS_2, because they reach a compromise between the deposition temperature and the quality of the as-deposited film. The adverse effect of low temperature reaction (lower than 200°C) is a tremendous decrease of crystallinity.

2.2 Self-limiting surface reaction

The underlying foundation of ALD is its self-limiting surface reaction, which makes it to be a surface-controlled method instead of a CVD related source-controlled method [59,60]. In a self-limiting surface reaction, the gaseous molecules are adsorbed on the surface of a solid substrate, including physical adsorption and chemical adsorption determined by the type of ALD process [59]. The thermal ALD is one of the energy-enhanced ALD processes whose advantage is that it can fulfill the requirement of self-terminating reactions on the surface of the complex 3D structure. Although each one has its individual features, most of thermal ALD reactions usually can refer to the classical technologies used in the precursor group of $Al(CH_3)_3/H_2O$ [61].

Following the pioneering work of Tan et al. [16], more and more researchers apply $MoCl_5/H_2S$ pairs as common precursors to ALD deposited MoS_2 film on the different substrates. However, the precursor adsorption mechanism is only illustrated by a scheme without specific supporting experimental data in this article. Subsequently, in work presented by Jin et al. [25], the self-limiting chemisorption is firstly confirmed by two functions between the thickness of the film (deposited with 100 cycles at 100°C) and the exposure time of the precursors ($Mo(CO)_6$ and CH_3SSCH_3), respectively. When the exposure time of the precursors is longer than a definite value (for $Mo(CO)_6$ is 3 s and for CH_3SSCH_3 is 0.5 s) [25], the adsorption sites of precursors on the substrate surface will reach saturation. In other words, the thickness of the film is no longer changing. Besides, some similar half-reactions have been proved in other ALD-made MoS_2 practices by using various precursors, such as $Mo(CO)_6/H_2S$ [47], $Mo(CO)_6/H_2S$ plasma [48], $Mo(thd)_3/H_2S$ [53], $Mo(NMe_2)_4/H_2S$ [21], MoF_6/H_2S [54], and $(N^tBu)_2(NMe_2)_2Mo/(CH_3)(CH_2)_2SH$ [58]. The adsorption state of the precursors can be indirectly estimated by monitoring the film thickness in these experiments, which indicates that the adsorption sites of the substrate can be fully occupied by precursors at a saturation state.

Although the state of adsorption can be determined by the experimental data, the detailed self-limiting surface reaction pathway of ALD deposited MoS_2 is not distinctly revealed. Commonly, the research on the reaction pathway requires using the *in-situ* characterization techniques, but the literature about the surface reaction pathway of ALD MoS_2 is still scarce currently. Fortunately, there are some articles using the density functional theory (DFT) simulation to help us figure out the self-limiting surface reaction pathway of the ALD synthesis MoS_2 process, which can provide insightful information. For example, the self-limiting surface reaction pathway of ALD synthesized MoS_2 on $SiO_2(0001)$ surface using $Mo(NMe_2)_2(N^tBu)_2$ and H_2S precursor is investigated by DFT [40]. Firstly, the Mo precursor is only physically adsorbed on the fully hydroxylated SiO_2, which means there are not chemical bonds between the precursors and the terminal OH groups on the surface of SiO_2. Then, the proton on a terminal OH group of SiO_2 is transferred to the N atom of the dimethylamido (NMe_2) ligand to produce chemical adsorption of protonated precursors, and sequentially the dimethylamine is desorbed (Figure 2(a)) [40]. After introducing the H_2S precursor, the dissociation of H_2S on the partially protonated ligand can produce the *tert*-butylamine (HN^tBu) desorption (Figure 2(b)). A complete coordinate Mo atom with terminal SH groups on the surface of SiO_2 is configured after the first ALD cycle. Besides, the increases in deposition temperature and H_2S pressure can cause a bigger H_2S dissociation rate and impingement rate, which can further enhance the desorption of *tert*-butylamine. By using DFT simulation, the adsorption of precursor molecules, the process of proton transfer, and the desorption of ligands can be clearly demonstrated.

Generally, the Mo precursor firstly reaches onto the substrate surface, then the S precursor follows as the co-reagent in the next exposure. The Mo precursor molecules are directly adsorbed on the active sites on the substrate surface, which is the first half-reaction and the starting point of the MoS_2 nucleus. However, H_2S as the most commonly used S precursor can decompose in H and SH groups, which will

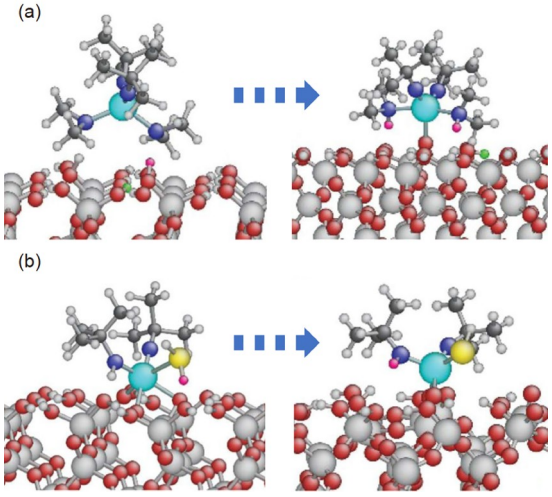

Figure 2 (Color online) (a) The adsorption process of the Mo precursor at the initial ALD cycle. (b) The dissociation of the S precursor at the initial ALD cycle. Reprinted with permission from ref. [40], Copyright 2018, the Royal Society of Chemistry.

decompose on the surface adsorbed by the Mo precursor.

At present, the decomposition of H_2S precursor can also be studied through theory. For example, the H_2S adsorption and decomposition processes on three different surfaces of α-quartz SiO_2 (cleaved O-terminated, dense O-terminated, and fully hydroxylated) have been studied by DFT [62]. According to theoretical calculations, the SiO_2 surface with the dense and fully hydroxylated is hard to adsorb chemically with H_2S, but the cleaved surface is highly reactive. It is an exothermic reaction process between the H_2S molecules and the cleaved O-terminated surface; consequently, the as-adsorbed H_2S is effortlessly dissociated into SH and H groups. The SH and H groups on the surface can constitute three configurations, including the H-terminal surface (configuration II and III) and S-terminal surface (configuration IV) (Figure 3(a)). The number of configuration IV is the most of the H_2S adsorption sites at low temperatures, but the number of configuration II and III is increased as the temperature increases (Figure 3(b), (c)).

Besides, an ALD surface reaction will become more complicated after H_2S is introduced. For example, Zhao et al. [63,64] report that the reaction pathway of the heterogeneous deposition stage (the initial ALD growth stage) is quite distinctive from that in the homogeneous deposition stage (the stable film growth stage) when the H_2S has been introduced. In the heterogeneous deposition stage, the conversion from Ni−O to NiS in the H_2S half-reaction is followed by the spontaneous aggregation of Ni-containing species with ligand stripped to form NiS clusters on the surface of the substrate. In the homogeneous deposition stage, the production of a sulfhydryl-amidine acid-base complex during the H_2S half-reaction on the substrate surface could create steric hindrance, which would result in a decrease in the growth rate of ALD films. In addition, the H_2S precursor has been replaced by an organosulfur compound of di-*tert*-butyl disulfide (TBDS) in ALD of nickel sulfide films [65], in which an ideal self-limiting surface reaction has been found. Although an analogous chemical has been recently used for the ALD MoS_2 [25], there is still a lack of relevant mechanism studies of ALD deposited MoS_2.

According to the above discussion, the OH groups on the surface of a substrate are more likely to adsorb to the Mo precursor molecules and are difficult to react with H_2S. This means that controlling the OH groups on the substrate surface will be a powerful method for controlling the growth process of ALD synthesized MoS_2. Plasma treatment, as an effective surface treatment tool, can controllably modify the number of OH groups on the surface of the substrate, which can facilitate the deposition of MoS_2 by the ALD process [28].

Generally, the functional groups on the surface, the partial pressure of precursors, and reaction conditions of ALD process can affect the self-limiting surface reaction, as well as the initial nucleation. Furthermore, steric hindrance can control the saturation of chemisorption, which prevents the formation of a full monolayer per precursor pulse. After Mo

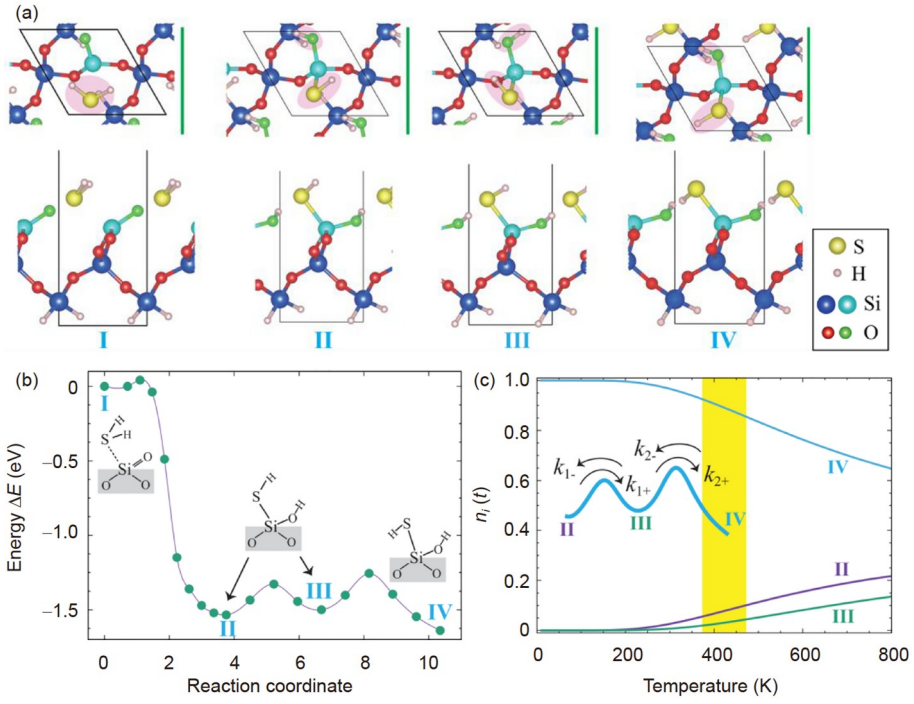

Figure 3 (Color online) (a) Top and side views and (b) the activation energy of H_2S adsorbed (I) and dissociative adsorption process (II–IV) on the α-quartz SiO_2 surface. (c) The temperature dependence of configuration II, III, IV sites. Reprinted with permission from ref. [62], Copyright 2018, American Institute of Physics.

precursor molecules chemisorb on the substrate surface, the ligands bind to the metal atom covers the hydroxyl groups on the subsurface, thus the hindered hydroxyl groups do not react during the growth process [61]. This will prevent the active sites on the surface from reaching the saturation state so that it is not conducive to the next ALD reaction. However, the complete steric hindrance effect in the manufacturing process of ALD deposited MoS_2 film is still open.

2.3 Growth mechanisms

Two possible growth mechanisms of ALD to prepare MoS_2 film are proposed experimentally. For the first type of growth mechanism, amorphous MoS_2 film deposited by ALD is annealed to obtain the desired MoS_2 with a layered structure. On the basis of the DFT simulation, an amorphous MoS_2 layer is formed on the SiO_2 substrate surface during the heterogeneous deposition stage [66], in which the building blocks created by the ALD self-limiting surface reaction have coalesced. In this buffer-layer, The O atoms on the surface of the SiO_2 substrate and the Mo atoms are connected by covalent bonds. The mismatch between the as-deposited MoS_2 after the heterogeneous stage and the crystalline SiO_2 surface is the key cause for the formation of the amorphous buffer-layer [66]. Under an ideal situation, there are 28 Mo atoms on the slab, but there are only 9 Mo atoms on this surface area in the amorphous buffer-layer (Figure 4(a)). The amorphous buffer layer could be extended along the *z*-direction through a different number of ALD cycles, or could be transformed into the crystalline MoS_2 layer after post-deposition annealing in a sulfur-containing atmosphere.

There are some reports on the amorphous MoS_2 layer in refs. [16,21,27,58], in which a post-annealing process can

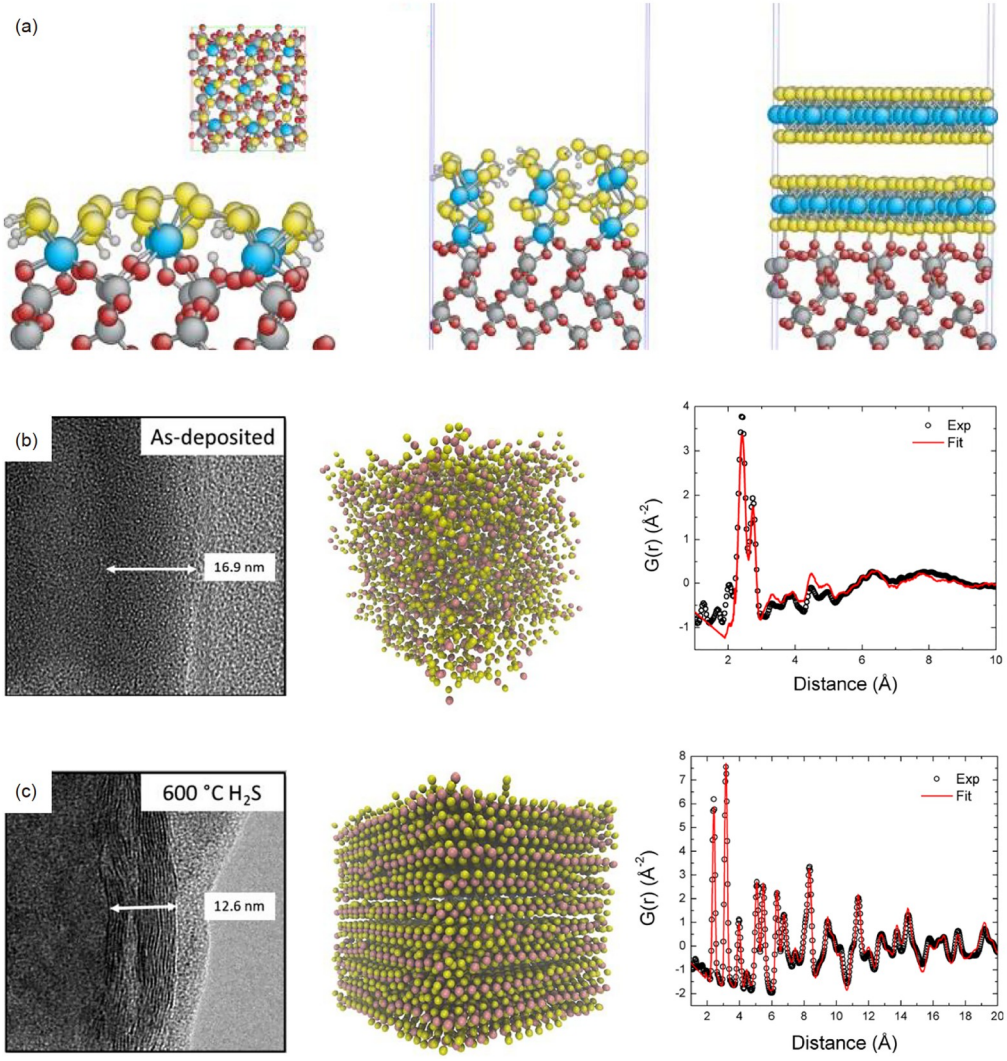

Figure 4 (Color online) (a) The formation process of a layer crystalline MoS_2 using annealing after several ALD cycles. Reprinted with permission from ref. [66]. Copyright 2018, American Institute of Physics. TEM image, simulated model image, and the corresponding associated normalized pair distributions functions of (b) 50 ALD cycles of as-deposited MoS_2 film and (c) the as-deposited film with 600°C H_2S annealing. Reprinted with permission from ref. [22], Copyright 2018, American Chemical Society.

promote the crystallinity of the MoS_2 films. Experimental data show that the crystallinity of as-deposited amorphous MoS_2 film annealed in H_2S environments is better than in H_2 environments [22] when the samples are annealed at the same temperature (at 400, 600°C, respectively). At the same time, the crystallinity of MoS_2 film is also improved with the temperature increasing (Figure 4(b), (c)).

As the development of this domain, a new growth mechanism based on the island has been progressively proposed [23,30,67]. Firstly, the nuclei of MoS_2 are formed in the initial ALD growth stage. Immediately, the crystal nuclei will grow into MoS_2 islands (Figure 5). Then, the size of the islands will grow up along the horizontal direction of the substrate surface. When the discrete MoS_2 islands coalesce, the grain boundary acts as the nucleation site for the formation of the next layer. The growth model of the top MoS_2 layer is converted from in-plane mode to out-of-plane mode, as the number of MoS_2 layers increases. The MoS_2 film deposited by ALD ultimately emerges to highly textured and perpendicular to the substrate surface (Figure 6).

MoS_2 islands firstly grow along the in-plane orientation owing to the dangling bonds at the edge of the MoS_2 layer, which play as active sites for the precursor adsorption. Due to the inconsistency of the crystal orientation along with in-plane orientation, defect sites will be generated at the junction of the grain boundaries. A new MoS_2 crystal layer will be formed on these defect sites at the edge. Moreover, the growth in the direction perpendicular to the substrate surface is slower than the growth along the edges of the MoS_2 islands. MoS_2 layers grow randomly in the out-of-plane orientation due to crowding effects between the grains [30].

The type of growth mechanisms can be determined by the actual experimental conditions, such as the type of precursors, the coverage of functional groups, and reactor conditions of the ALD process. When the deposition temperature is less than 200°C, it is usually the first type [68]. As the deposition temperature increases, the growth mechanism will transfer to the second growth type. No matter what type of growth mechanism, the growth process of ALD to prepare MoS_2 film consists of two stages, heterogeneous deposition stage and homogeneous deposition stage. The heterodeposition is the process by which the precursors are adsorbed on the surface of the substrate at the initial ALD cycles. The homodeposition is the process of adsorbing the precursor on the surface of MoS_2 obtained by the heterodeposition. In heterodeposition, the self-limiting surface reaction will be contributed by the adsorption between the precursor molecules and the OH groups on the surface. In homodeposition, the main active site is transferred to the S and SH functional groups, which will adsorb the incoming precursors. Usually, the growth rate of the homodeposition stage is faster than that of the heterodeposition stage [66], which conduces the difficulty for ALD to control the growth of MoS_2.

An underlying difference between the two growth mechanisms is the formation time of the crystalline layer of MoS_2. For the first type, the crystalline layer of MoS_2 is formed after annealing, whereas the crystalline layer has been formed at the initial stage of ALD deposited MoS_2 film for the second type. In other words, the amorphous structure can spread along the parallel and perpendicular direction to the substrate surface in the first type. But the crystalline layer of MoS_2 grows only along the lateral direction in the second type. If grains oriented in the same direction can be obtained by tuning the growth process, these grains should be able to coalesce with each other to form a larger single crystal according to the second growth mechanism. For example, Mattinen et al. [69] researched the crystal orientation of MoS_2 multilayer films deposited by ALD on the sapphire, mica, and SiO_2/Si substrates. The 2H phase MoS_2 only exhibits van der Waals epitaxial growth on the mica, but it is fiber texture growth on the other two substrates. For the

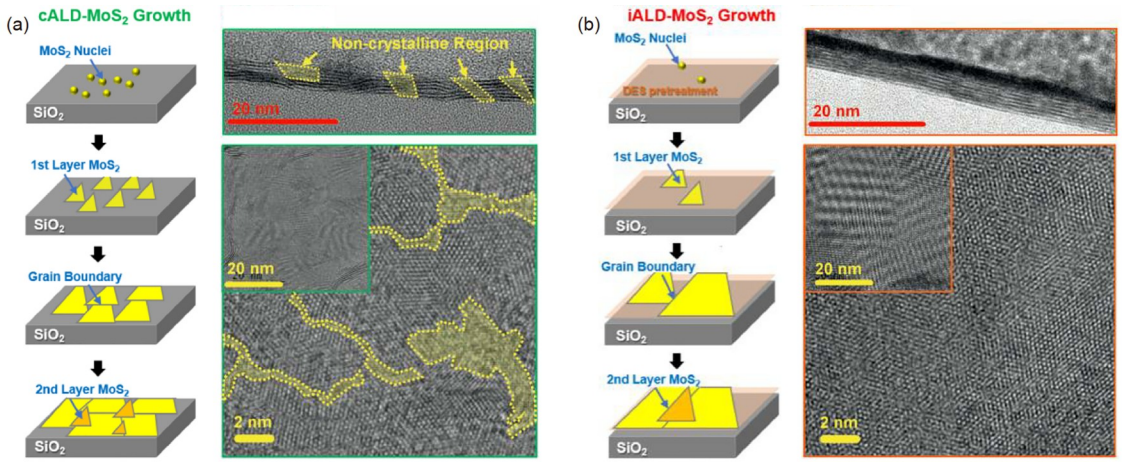

Figure 5 (Color online) The growth models and corresponding TEM images of MoS_2 film deposited by (a) the conventional ALD and (b) the inhibitor-utilizing ALD. Reprinted with permission from ref. [23], Copyright 2017, John Wiley and Sons.

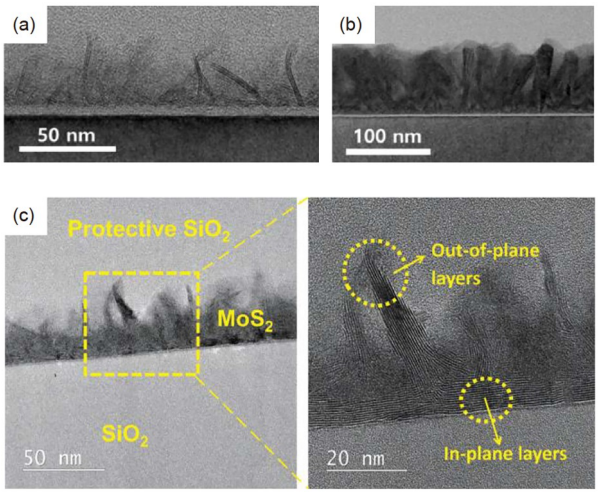

Figure 6 (Color online) Cross-sectional TEM images of MoS_2 film using (a) 300 ALD cycles and (b) 1000 ALD cycles (250–300°C) on p-type silicon substrate (Reprinted with permission from ref. [67], Copyright 2018, Multidisciplinary Digital Publishing Institute). (c) Cross-sectional TEM images and the corresponding magnified view of MoS_2 film using 200 ALD cycles (450°C) on SiO_2/Si substrate (Reprinted with permission from ref. [30], Copyright 2018, Royal Society of Chemistry).

MoS_2 deposited on the mica, the main epitaxial relation is [1 $\bar{2}$ 1 0] or [2 $\bar{1}$ $\bar{1}$ 0] MoS_2 || [1 0 0] mica (0°/60°) and [0 $\bar{1}$ 1 0] or [1 $\bar{1}$ 0 0] MoS_2 || [1 0 0] mica (30°/90°). Therefore, it is necessary to further tune the growth conditions to decrease the number of the epitaxial direction, contributing to the fusion of grains. This will be quite interesting and potentially useful.

In addition, it can be deduced from this growth mechanism that the nucleation density at the heterogeneous deposition stage could affect the formation of the first MoS_2 layer, which can be proved in refs. [23,70]. A decreasing nucleation density could provide a more horizontal growth area at the initial ALD stage, which will increase the grain size of MoS_2. However, it is still a significant challenge to obtain the centimeter length scale of MoS_2 grains (the level of CVD MoS_2) by using ALD [71]. Until now, ALD is usually used to fabricate MoS_2 with out-of-plane orientation, which has an excellent catalytic performance [30,72–77]. The out-of-plane standing structures of MoS_2 deposited by ALD can be evidently observed by TEM images (Figure 6). Additionally, the polarized Raman spectroscopy as a non-destructive technique can rapidly elucidate the texture of MoS_2 films [78].

2.4 Extension of ALD technique

Almost all the early literature on ALD manufacturing MoS_2 films is based on the binary ALD process. As the progress of this field, there are two main efforts in the extension of as-deposited MoS_2 film by ALD, inside the ALD chamber and outside the ALD chamber. Some new deposition strategies of the inside chamber, such as pretreatment of the substrate surface and dispersing the precursor flow, can improve the crystallinity of as-deposited MoS_2. Some strategies of the outside chamber, such as the ternary ALD process, can extend the application of MoS_2 film.

The strategies of the inside chamber can influence the growth process of MoS_2 film. For example, pretreatment of the substrate surface and dispersing the precursor flow can decrease nucleation density, which strongly affects not only the grain size of MoS_2 film formed by the first layer but also the formation of the following MoS_2 layers. For example, an inhibitor-utilizing ALD process of synthesizing MoS_2 to achieve nucleation control has been reported by Jeon et al. [23]. The O-S or O-C bonds will be produced at the surface when the surface of SiO_2 substrate is pretreated with diethyl sulfide (DES). Compared with the DES pretreated surface, the Mo precursor is easier to adsorb on the pristine SiO_2 surface by the production of Mo-O bond. The reaction energy between the Mo precursor and the DES pretreated surface (+1.75 eV) is much greater than that between the Mo precursor and the pristine SiO_2 surface (−0.92 eV), which means that DES could passivate the active sites by forming stable C-O bonds, inhibiting the adsorption of Mo precursors. Therefore, DES inhibitors can decrease the nucleation density.

For another example, a trickle flow ALD process for reducing the nucleation density has been reported by Yang and Liu [70]. The precursor airstream is dispersed into a trickle-fluidization gas current by a Ni foam on top of the sample. This strategy of trickle-fluidization precursor flow can reduce the precursors that reach the substrate per unit time. Few precursors can effectively decrease the nucleation density and increase the lateral space of grains, increasing the size of grains.

More complex TMDs materials, such as ternary materials, cannot be synthesized directly through a binary ALD process, but they can be synthesized by a supercycle ALD process [41]. For example, a ternary ALD process is firstly introduced to synthesize MoS_2/ReS_2 heterojunctions by Liu et al. [79]. MoS_2/ReS_2 heterojunctions manufactured by ALD, a bimetallic co-chamber feeding ALD process, have a controllable Mo/Re ratio (Figure 7(a)–(d)). The formation mechanism of the in-plane MoS_2/ReS_2 heterojunction is that the precursors of $MoCl_5$ and $ReCl_5$ may not be completely mixed. Furthermore, Lv et al. [80] deposited the MoS_2/ReS_2 heterojunction film on the AFM tip by using the same ALD process (Figure 7(e)–(h)). By controlling the thickness of the MoS_2/ReS_2 heterojunction film deposited on the AFM tip, the adhesion between the tip and the surface of the substrate can be adjusted, which is between 13.5 and 136.3 nN. AFM tip is a powerful tool for exploring nanoworld. Therefore, AFM tip modified by ultrathin heterojunction films may be an important potential tool in the practice of science and

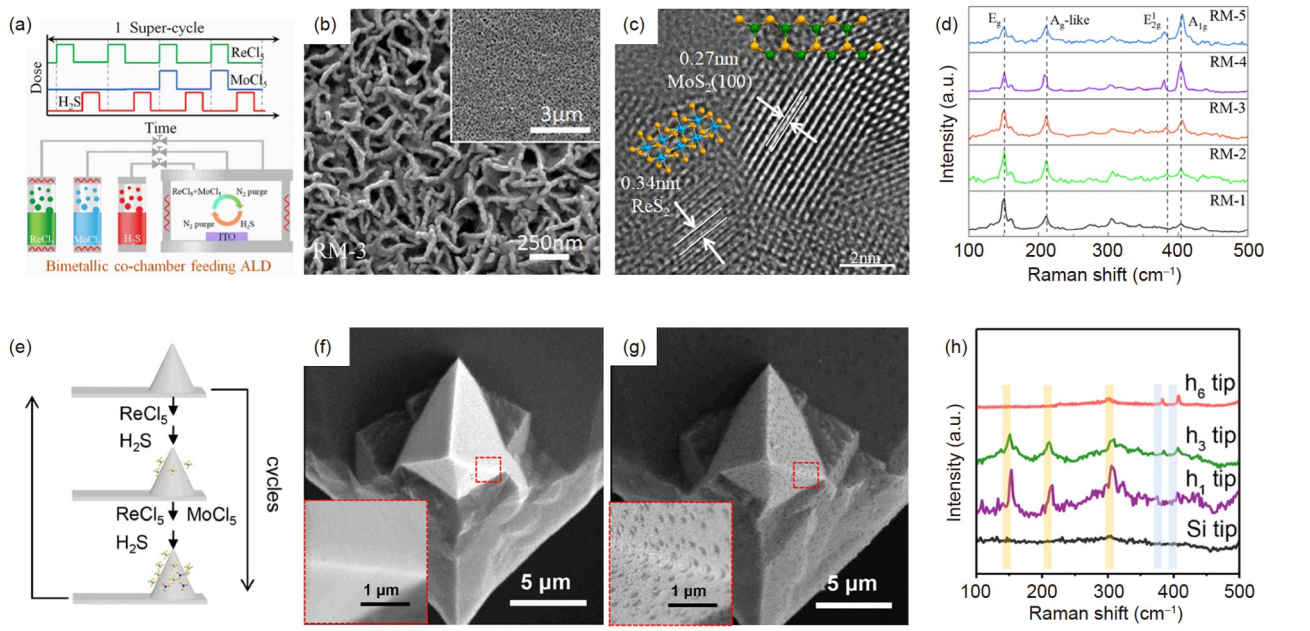

Figure 7 (Color online) (a) Schematic illustration of the bimetallic co-chamber feeding ALD, (b) SEM images of MoS_2/ReS_2 heterojunctions (RM-3), (c) the HRTEM image of the corresponding sample, (d) Raman spectra of the samples with different Mo/Re ratio (reprinted with permission from ref. [79], Copyright 2019, American Chemical Society). (e) Schematic illustration of preparation process of depositing heterojunction film on the AFM tip, the SEM images of (f) pristine Si tip and (g) the tip covered with heterojunction film, (h) Raman spectra of the tips coated MoS_2 with different Mo/Re ratio (reprinted with permission from ref. [80], Copyright 2020, American Chemical Society).

technology innovation.

3 Applications

The applications of ALD deposited MoS_2 are usually the extension of the growth mechanism. ALD deposited MoS_2 film has attracted enormous attention from the fields of batteries [43,46,56,81], supercapacitors [49], electronics [5,6,23,44,52,82], catalysis [27,30,51,72–75,77,83], and lubrication [48,84]. Although the fields of application are wide (Table 2), these applications essentially utilize the characteristics of self-limiting surface reaction, which makes it possible to fabricate thickness controlled, uniform, and conformal MoS_2 film. For the feature of thickness control, the growth rate (growth thickness of MoS_2 film deposited in one ALD cycle) is a linear relationship [25,58]. This means that the number of ALD cycles can simply precisely control the film thickness in an ALD process. The uniformity of film usually means having the same composition, thickness, and physical properties at each point on the surface of a planar substrate. [18]. For example, the MoS_2 film can be uniformly grown on the wafer-scale (4-inch in diameter, 1 inch=2.54 cm) [47,48,85]. However, large area uniform MoS_2 film without damaging a pristine structure using the ALD process still needs to be further researched.

The most special feature of the ALD deposited MoS_2 process is ~100% conformality, which means that the as-deposited MoS_2 film has equal thickness and properties for the surface of the 3D complex structures with a large aspect ratio [18]. For example, the MoS_2 films are deposited on single-crystalline CdS nanorod arrays by the ALD process [74]. Besides, more structures with high aspect ratio have been reported in the literature (Figure 8), such as anodic aluminum oxide [86], porous TiO_2 inverse opals [87], 3D foam [49,77], nanotube [56,57,72,75,81], and carbon fiber paper [73]. MoS_2 is deposited on these structures by ALD to improve the performance of MoS_2.

4 Summary and outlook

Although ALD-made MoS_2 has some problems such as nucleation and crystallinity, the ALD technique proves to be efficient for preparing controlled MoS_2 films. So far, the nucleation process of ALD deposited MoS_2 film is only demonstrated through DFT theoretical calculation. The nucleation process includes the adsorption of precursor molecules, the transformation of the proton, and the desorption of the protonated ligands, and these processes need further support using *in-situ* characterization techniques. The reactor conditions, the functional groups, and the partial pressure will affect the nucleation in the initial ALD cycles in actual experiments. Besides, the precursor gas transmission mode in the high aspect ratio structure is determined by the partial pressure of the precursor, which further affects the conformal coating process in the ALD process. Currently, although the crystallinity of MoS_2 film deposited by ALD is still poor, it

Table 2 Summary about substrates and applications for MoS_2 film deposited by ALD

Substrate	Thickness of MoS_2	Application	Characteristics	Ref.
Sapphire	0.6–3.2 nm	–	2-inch	[16]
Sapphire	25–30 nm	Na-ion battery	Capacity: 1710 mA h g^{-1}	[43]
Sapphire	2–9 nm	Transistor arrays	On/off current ratio: 10^3 Mobility: 11.56 $cm^2 V^{-1} s^{-1}$	[52]
Sapphire	~2.8 nm	Switching and sensing devices	On/off current ratio: ~5×10^2	[44]
SiO_2	5–27.5 nm	–	4-inch	[48]
SiO_2	0–25 nm	–	4-inch	[47]
SiO_2	2–3 layers	–	150 mm	[85]
Carbon fiber papers	2.6–14 nm	Electrochemical hydrogen evolution	Tafel slope: 56.6–55.6 mV dec^{-1}; Overpotential: 220 mV	[51]
Carbon fiber paper	28–60 nm	Electrochemical oxygen evolution	Tafel slope: 65.8 mV dec^{-1}; Overpotential: 311 mV	[73]
Si/Si_3N_4	10 nm	Photolithographic and lift-off patterning	–	[21]
TiO_2 inverse opals	20 nm	–	–	[87]
3D Ni foam	10 nm	Supercapacitor	Areal capacitance: 3400 mF cm^{-2}	[49]
Si photocathodes	14 nm	Photoelectrochemical water reduction reaction	Photocurrent density: 21.7 mA cm^{-2}	[27]
Cobalt foam	–	Electrochemical oxygen evolution	Current density: 10 mA cm^{-2}; Overpotential: 270 mV;	[77]
Titania nanotube array	7.5–20 nm	Hydrogen evolution reaction	Current density: 50 mA cm^{-2}	[75]
CdS nanorod array	7 nm	Photoelectrochemical	Photocurrent density: 1.9 mA cm^{-2}	[74]
TiO_2 nanotube	–	Photocatalysis	–	[72]
TiO_2 nanotube	–	Electrochemical	Coulombic efficiency: 98%	[56]
Anodic aluminum oxide nanochannel	–	Ultrasensitive detection	The detection limit of miRNA-155: 3 aM	[86]
Carbon nanotube	~5 nm	Li-O_2 batteries	Capacity: 4844 mA h g^{-1}	[81]
Gold pads	2.76–17.9 nm	–	–	[45]

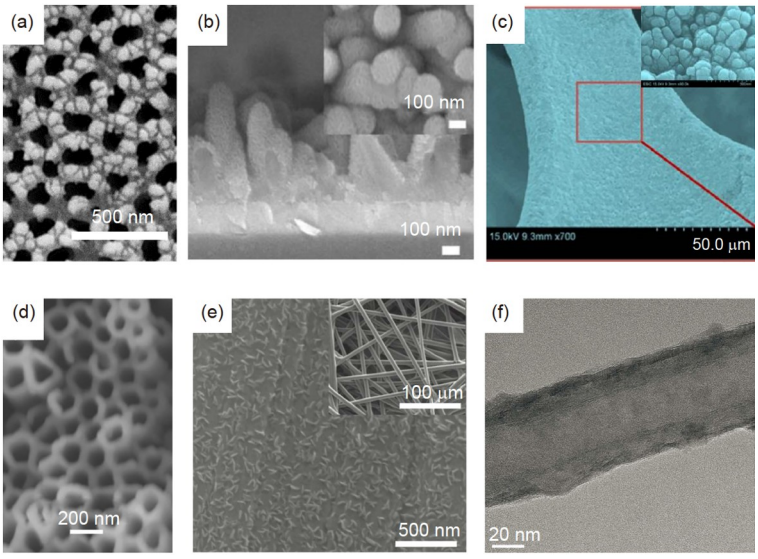

Figure 8 (Color online) SEM images of MoS_2 deposited on (a) anodic aluminum oxide, (b) CdS nanorod arrays, (c) 3D-Ni-foam, (d) TNTAs, (e) CFP, and TEM image of MoS_2 deposited on (f) CNT. Reprinted with permission from ref. [86], Copyright 2020, John Wiley and Sons. Ref. [74], Copyright 2019, American Chemical Society. Ref. [49], Copyright 2017, American Chemical Society. Ref. [75], Copyright 2019, American Chemical Society. Ref. [73], Copyright 2019, Institute of Physics. Ref. [57], Copyright 2020, Royal Society of Chemistry.

can be improved by some technique-level methods such as PEALD, post-deposition annealing, and the method combined ALD and CVD. In addition, some mechanism-level methods have also been used to promote the crystallinity of MoS_2, for example, decreasing the nucleation density in the initial ALD stage. If the crystallinity of MoS_2 film is expected to be completely solved, the mismatch between the as-deposited MoS_2 in the heterodeposition and the surface of the substrate needs to be solved first.

In addition, area-selective ALD may offer another opportunity in the synthesis of 2D MoS_2 with atomic-level precision. Area-selective ALD can limit the lateral arrangement of the atoms by the differences in local self-limiting surface reaction, which can pattern the ALD-grown films. Previous work about ALD prepared MoS_2 has focused on the controlled thickness deposition on the entire surface. Area-selective ALD is expected to break through this limitation, which is considered as a step toward using atoms as building blocks for synthesizing 2D MoS_2. Recently, atomic layer etching (ALE), as a variation of the ALD process, has been introduced for preparing 2D TMDs. The forthright way to combine the ALE process and area-selective ALD is to develop a supercycle program. Furthermore, the supercycle ALD approach combined with binary ALD cycles can be used to synthesize more complex TMDs materials.

Currently, ALD deposited MoS_2 film has been mainly applied in the domains of electronics and energy, as-deposited MoS_2 film has also been used to manufacture biosensor devices. Due to the numerous advantages of ALD-made MoS_2 film, it can be expected that MoS_2 film obtained in ALD will be utilized in more domains, such as surface-enhanced Raman scattering.

This work was supported by the National Natural Science Foundation of China (Grant No. 51822501), the Natural Science Foundation of Jiangsu Province (Grant Nos. BK20170023, BK20181274), the Fundamental Research Funds for the Central Universities (Grant Nos. 3202006301, 3202006403), the Qing Lan Project of Jiangsu Province, the International Foundation for Science, Stockholm, Sweden, the Organization for the Prohibition of Chemical Weapons, The Hague, Netherlands, through a grant to Lei Liu (F/4736-2), the grants from Top 6 High-Level Talents Program of Jiangsu Province (Grant No. 2017-GDZB-006, Class A), the Tribology Science Fund of State Key Laboratory of Tribology (Grant No. SKLTKF15A11), Open Research Fund of State Key Laboratory of High Performance Complex Manufacturing, Central South University (Grant No. Kfkt2016-11), Open Research Fund of State Key Laboratory of Fire Science (Grant No. HZ2017-KF05) and Open Research Fund of State Key Laboratory of Solid Lubrication (Grant No. LSL-1607).

1 Samadi M, Sarikhani N, Zirak M, et al. Group 6 transition metal dichalcogenide nanomaterials: Synthesis, applications and future perspectives. Nanoscale Horiz, 2018, 3: 90–204
2 Wang Q H, Kalantar-Zadeh K, Kis A, et al. Electronics and optoelectronics of two-dimensional transition metal dichalcogenides. Nat Nanotech, 2012, 7: 699–712
3 Singh A K, Kumar P, Late D J, et al. 2D layered transition metal dichalcogenides (MoS_2): Synthesis, applications and theoretical aspects. Appl Mater Today, 2018, 13: 242–270
4 Radisavljevic B, Radenovic A, Brivio J, et al. Single-layer MoS_2 transistors. Nat Nanotech, 2011, 6: 147–150
5 Ahn W, Lee H, Cho Y, et al. Introduction of an Al seed layer for facile adsorption of $MoCl_5$ during atomic layer deposition of MoS_2. Phys Status Solidi A, 2020, 217: 1901042
6 Liu H, Chen L, Zhu H, et al. Atomic layer deposited 2D MoS_2 atomic crystals: From material to circuit. Nano Res, 2020, 13: 1644–1650
7 Mak K F, He K, Shan J, et al. Control of valley polarization in monolayer MoS_2 by optical helicity. Nat Nanotech, 2012, 7: 494–498
8 Singh E, Kim K S, Yeom G Y, et al. Atomically thin-layered molybdenum disulfide (MoS_2) for bulk-heterojunction solar cells. ACS Appl Mater Inter, 2017, 9: 3223–3245
9 Perkins F K, Friedman A L, Cobas E, et al. Chemical vapor sensing with monolayer MoS_2. Nano Lett, 2013, 13: 668–673
10 Kalantar-zadeh K, Ou J Z. Biosensors based on two-dimensional MoS_2. ACS Sens, 2016, 1: 5–16
11 Cao X, Gan X, Lang H, et al. Anisotropic nanofriction on MoS_2 with different thicknesses. Tribol Int, 2019, 134: 308–316
12 Hao W, Marichy C, Journet C. Atomic layer deposition of stable 2D materials. 2D Mater, 2018, 6: 012001
13 Mak K F, Lee C, Hone J, et al. Atomically thin MoS_2: A new direct-gap semiconductor. Phys Rev Lett, 2010, 105: 136805
14 Lee Y H, Zhang X Q, Zhang W, et al. Synthesis of large-area MoS_2 atomic layers with chemical vapor deposition. Adv Mater, 2012, 24: 2320–2325
15 Kang K, Xie S, Huang L, et al. High-mobility three-atom-thick semiconducting films with wafer-scale homogeneity. Nature, 2015, 520: 656–660
16 Tan L K, Liu B, Teng J H, et al. Atomic layer deposition of a MoS_2 film. Nanoscale, 2014, 6: 10584–10588
17 Lu J, Elam J W, Stair P C. Atomic layer deposition—Sequential self-limiting surface reactions for advanced catalyst "bottom-up" synthesis. Surf Sci Rep, 2016, 71: 410–472
18 Cremers V, Puurunen R L, Dendooven J. Conformality in atomic layer deposition: Current status overview of analysis and modelling. Appl Phys Rev, 2019, 6: 021302
19 Kim H G, Lee H B R. Atomic layer deposition on 2D materials. Chem Mater, 2017, 29: 3809–3826
20 Schwartzberg A M, Olynick D. Complex materials by atomic layer deposition. Adv Mater, 2015, 27: 5778–5784
21 Jurca T, Moody M J, Henning A, et al. Low-temperature atomic layer deposition of MoS_2 films. Angew Chem Int Ed, 2017, 56: 4991–4995
22 Letourneau S, Young M J, Bedford N M, et al. Structural evolution of molybdenum disulfide prepared by atomic layer deposition for realization of large scale films in microelectronic applications. ACS Appl Nano Mater, 2018, 1: 4028–4037
23 Jeon W, Cho Y, Jo S, et al. Wafer-scale synthesis of reliable high-mobility molybdenum disulfide thin films via inhibitor-utilizing atomic layer deposition. Adv Mater, 2017, 29: 1703031
24 Shi M L, Chen L, Zhang T B, et al. Top-down integration of molybdenum disulfide transistors with wafer-scale uniformity and layer controllability. Small, 2017, 13: 1603157
25 Jin Z, Shin S, Kwon D H, et al. Novel chemical route for atomic layer deposition of MoS_2 thin film on SiO_2/Si substrate. Nanoscale, 2014, 6: 14453–14458
26 Cadot S, Renault O, Frégnaux M, et al. A novel 2-step ALD route to ultra-thin MoS_2 films on SiO_2 through a surface organometallic intermediate. Nanoscale, 2017, 9: 538–546
27 Oh S, Kim J B, Song J T, et al. Atomic layer deposited molybdenum disulfide on Si photocathodes for highly efficient photoelectrochemical water reduction reaction. J Mater Chem A, 2017, 5: 3304–3310
28 Yang J, Liu L. Nanotribological properties of 2-D MoS_2 on different substrates made by atomic layer deposition (ALD). Appl Surf Sci, 2020, 502: 144402

29 Mughal A J, Walter T N, Cooley K A, et al. Effect of substrate on the growth and properties of MoS_2 thin films grown by plasma-enhanced atomic layer deposition. J Vacuum Sci Tech A, 2019, 37: 010907
30 Sharma A, Verheijen M A, Wu L, et al. Low-temperature plasma-enhanced atomic layer deposition of 2-D MoS_2: Large area, thickness control and tuneable morphology. Nanoscale, 2018, 10: 8615–8627
31 Moody M J, Henning A, Jurca T, et al. Atomic layer deposition of molybdenum oxides with tunable stoichiometry enables controllable doping of MoS_2. Chem Mater, 2018, 30: 3628–3632
32 Graniel O, Weber M, Balme S, et al. Atomic layer deposition for biosensing applications. Biosens Bioelectron, 2018, 122: 147–159
33 Singh E, Singh P, Kim K S, et al. Flexible molybdenum disulfide (MoS_2) atomic layers for wearable electronics and optoelectronics. ACS Appl Mater Inter, 2019, 11: 11061–11105
34 Krishnan U, Kaur M, Singh K, et al. A synoptic review of MoS_2: Synthesis to applications. Superlattices Microstruct, 2019, 128: 274–297
35 Bazaka K, Levchenko I, Lim J W M, et al. MoS_2-based nanostructures: Synthesis and applications in medicine. J Phys D-Appl Phys, 2019, 52: 183001
36 Nam T, Seo S, Kim H. Atomic layer deposition of a uniform thin film on two-dimensional transition metal dichalcogenides. J Vacuum Sci Tech A, 2020, 38: 030803
37 Cai J, Han X, Wang X, et al. Atomic layer deposition of two-dimensional layered materials: Processes, growth mechanisms, and characteristics. Matter, 2020, 2: 587–630
38 Manzeli S, Ovchinnikov D, Pasquier D, et al. 2D transition metal dichalcogenides. Nat Rev Mater, 2017, 2: 17033
39 Hagen D J, Pemble M E, Karppinen M. Atomic layer deposition of metals: Precursors and film growth. Appl Phys Rev, 2019, 6: 041309
40 Shirazi M, Kessels W M M, Bol A A. Initial stage of atomic layer deposition of 2D-MoS_2 on a SiO_2 surface: A DFT study. Phys Chem Chem Phys, 2018, 20: 16861–16875
41 Mackus A J M, Schneider J R, MacIsaac C, et al. Synthesis of doped, ternary, and quaternary materials by atomic layer deposition: A review. Chem Mater, 2019, 31: 1142–1183
42 Huang Y, Liu L, Zhao W, et al. Preparation and characterization of molybdenum disulfide films obtained by one-step atomic layer deposition method. Thin Solid Films, 2017, 624: 101–105
43 Sreedhara M B, Gope S, Vishal B, et al. Atomic layer deposition of crystalline epitaxial MoS_2 nanowall networks exhibiting superior performance in thin-film rechargeable Na-ion batteries. J Mater Chem A, 2018, 6: 2302–2310
44 Tian Z L, Zhao D H, Liu H, et al. Optimization of defects in large-area synthetic MoS_2 thin films by CS_2 treatment for switching and sensing devices. ACS Appl Nano Mater, 2019, 2: 7810–7818
45 Yue C, Wang Y, Liu H, et al. Controlled growth of MoS_2 by atomic layer deposition on patterned gold pads. J Cryst Growth, 2020, 541: 125683
46 Nandi D K, Sen U K, Choudhury D, et al. Atomic layer deposited MoS_2 as a carbon and binder free anode in Li-ion battery. Electrochim Acta, 2014, 146: 706–713
47 Pyeon J J, Kim S H, Jeong D S, et al. Wafer-scale growth of MoS_2 thin films by atomic layer deposition. Nanoscale, 2016, 8: 10792–10798
48 Jang Y, Yeo S, Lee H B R, et al. Wafer-scale, conformal and direct growth of MoS_2 thin films by atomic layer deposition. Appl Surf Sci, 2016, 365: 160–165
49 Nandi D K, Sahoo S, Sinha S, et al. Highly uniform atomic layer-deposited MoS_2@3D-Ni-foam: A novel approach to prepare an electrode for supercapacitors. ACS Appl Mater Inter, 2017, 9: 40252–40264
50 Shin S, Jin Z, Kwon D H, et al. High turnover frequency of hydrogen evolution reaction on amorphous MoS_2 thin film directly grown by atomic layer deposition. Langmuir, 2015, 31: 1196–1202
51 Kwon D H, Jin Z, Shin S, et al. A comprehensive study on atomic layer deposition of molybdenum sulfide for electrochemical hydrogen evolution. Nanoscale, 2016, 8: 7180–7188
52 Zhang T, Wang Y, Xu J, et al. High performance few-layer MoS_2 transistor arrays with wafer level homogeneity integrated by atomic layer deposition. 2D Mater, 2018, 5: 015028
53 Mattinen M, Hatanpää T, Sarnet T, et al. Atomic layer deposition of crystalline MoS_2 thin films: New molybdenum precursor for low-temperature film growth. Adv Mater Interfaces, 2017, 4: 1700123
54 Mane A U, Letourneau S, Mandia D J, et al. Atomic layer deposition of molybdenum disulfide films using MoF_6 and H_2S. J Vacuum Sci Tech A, 2018, 36: 01A125
55 Kim Y, Choi D, Woo W J, et al. Synthesis of two-dimensional MoS_2/graphene heterostructure by atomic layer deposition using MoF_6 precursor. Appl Surf Sci, 2019, 494: 591–599
56 Sopha H, Tesfaye A T, Zazpe R, et al. ALD growth of MoS_2 nanosheets on TiO_2 nanotube supports. FlatChem, 2019, 17: 100130
57 Shen C, Raza M H, Amsalem P, et al. Morphology-controlled MoS_2 by low-temperature atomic layer deposition. Nanoscale, 2020, 12: 20404–20412
58 Kalanyan B, Beams R, Katz M B, et al. MoS_2 thin films from a $(N^tBu)_2(NMe_2)_2$ Mo and 1-propanethiol atomic layer deposition process. J Vacuum Sci Tech A, 2019, 37: 010901
59 Puurunen R L. Surface chemistry of atomic layer deposition: A case study for the trimethylaluminum/water process. J Appl Phys, 2005, 97: 121301
60 Puurunen R L. A short history of atomic layer deposition: Tuomo suntola's atomic layer epitaxy. Chem Vapor Depos, 2014, 20: 332–344
61 Guerra-Nuñez C, Döbeli M, Michler J, et al. Reaction and growth mechanisms in Al_2O_3 deposited via atomic layer deposition: Elucidating the hydrogen source. Chem Mater, 2017, 29: 8690–8703
62 Kim H J, Jeon H, Shin Y H. H_2S adsorption process on (0001) α-quartz SiO_2 surfaces. J Appl Phys, 2018, 124: 115301
63 Zhao R, Guo Z, Wang X. Surface chemistry during atomic-layer deposition of nickel sulfide from nickel amidinate and H_2S. J Phys Chem C, 2018, 122: 21514–21520
64 Zhao R, Wang X. Initial growth and agglomeration during atomic layer deposition of nickel sulfide. Chem Mater, 2019, 31: 445–453
65 Li H, Zhao R, Zhu J, et al. Organosulfur precursor for atomic layer deposition of high-quality metal sulfide films. Chem Mater, 2020, 32: 8885–8894
66 Shirazi M, Kessels W M M, Bol A A. Strategies to facilitate the formation of free standing MoS_2 nanolayers on SiO_2 surface by atomic layer deposition: A DFT study. APL Mater, 2018, 6: 111107
67 Joe J, Bae C, Kim E, et al. Mixed-phase (2H and 1T) MoS_2 catalyst for a highly efficient and stable Si photocathode. Catalysts, 2018, 8: 580
68 Huang Y, Liu L. Recent progress in atomic layer deposition of molybdenum disulfide: A mini review. Sci China Mater, 2019, 62: 913–924
69 Mattinen M, King P J, Popov G, et al. Van der Waals epitaxy of continuous thin films of 2D materials using atomic layer deposition in low temperature and low vacuum conditions. 2D Mater, 2020, 7: 011003
70 Yang J, Liu L. Trickle flow aided atomic layer deposition (ALD) strategy for ultrathin molybdenum disulfide (MoS_2) synthesis. ACS Appl Mater Inter, 2019, 11: 36270–36277
71 Lim Y F, Priyadarshi K, Bussolotti F, et al. Modification of vapor phase concentrations in MoS_2 growth using a NiO foam barrier. ACS Nano, 2018, 12: 1339–1349
72 Motola M, Baudys M, Zazpe R, et al. 2D MoS_2 nanosheets on 1D anodic TiO_2 nanotube layers: An efficient co-catalyst for liquid and gas phase photocatalysis. Nanoscale, 2019, 11: 23126–23131
73 Huang Y, Liu L, Liu X. Modulated electrochemical oxygen evolution catalyzed by MoS_2 nanoflakes from atomic layer deposition. Nanotechnology, 2019, 30: 095402
74 Ho T A, Bae C, Joe J, et al. Heterojunction photoanode of atomic-layer-deposited MoS_2 on single-crystalline CdS nanorod arrays. ACS Appl Mater Inter, 2019, 11: 37586–37594
75 Cao Y, Wu Y, Badie C, et al. Electrocatalytic performance of titania nanotube arrays coated with MoS_2 by ALD toward the hydrogen

evolution reaction. ACS Omega, 2019, 4: 8816–8823
76 MacIsaac C, Schneider J R, Closser R G, et al. Atomic and molecular layer deposition of hybrid Mo-thiolate thin films with enhanced catalytic activity. Adv Funct Mater, 2018, 28: 1800852
77 Xiong D, Zhang Q, Li W, et al. Atomic-layer-deposited ultrafine MoS_2 nanocrystals on cobalt foam for efficient and stable electrochemical oxygen evolution. Nanoscale, 2017, 9: 2711–2717
78 Vandalon V, Sharma A, Perrotta A, et al. Polarized Raman spectroscopy to elucidate the texture of synthesized MoS_2. Nanoscale, 2019, 11: 22860–22870
79 Liu L, Ma K, Xu X, et al. MoS_2-ReS_2 heterojunctions from a bimetallic co-chamber feeding atomic layer deposition for ultrasensitive MiRNA-21 detection. ACS Appl Mater Inter, 2020, 12: 29074–29084
80 Lv J, Yang J, Jiao S, et al. Ultrathin quasibinary heterojunctioned ReS_2/MoS_2 film with controlled adhesion from a bimetallic co-feeding atomic layer deposition. ACS Appl Mater Inter, 2020, 12: 43311–43319
81 Song M, Tan H, Li X, et al. Atomic-layer-deposited amorphous MoS_2 for durable and flexible Li-O_2 batteries. Small Methods, 2020, 4: 1900274
82 Zhang T, Liu H, Wang Y, et al. Fast-response inverter arrays built on wafer-scale MoS_2 by atomic layer deposition. Phys Status Solidi RRL, 2019, 13: 1900018
83 Ho T A, Bae C, Lee S, et al. Edge-on MoS_2 thin films by atomic layer deposition for understanding the interplay between the active area and hydrogen evolution reaction. Chem Mater, 2017, 29: 7604–7614
84 Huang Y, Liu L, Yang J, et al. Nanotribological properties of ALD-made ultrathin MoS_2 influenced by film thickness and scanning velocity. Langmuir, 2019, 35: 3651–3657
85 Valdivia A, Tweet D J, Conley John F. J. Atomic layer deposition of two dimensional MoS_2 on 150 mm substrates. J Vacuum Sci Tech A, 2016, 34: 021515
86 Jiao S, Liu L, Wang J, et al. A novel biosensor based on molybdenum disulfide (MoS_2) modified porous anodic aluminum oxide nanochannels for ultrasensitive microRNA-155 detection. Small, 2020, 16: 2001223
87 Li X, Puttaswamy M, Wang Z, et al. A pressure tuned stop-flow atomic layer deposition process for MoS_2 on high porous nanostructure and fabrication of TiO_2/MoS_2 core/shell inverse opal structure. Appl Surf Sci, 2017, 422: 536–543